Journal of
Translational Regenerative Medicine

2026. Volume 1

Research Paper

Comparative Study of Chitosan/Hyaluronic Acid Modified Injectable Calcium Phosphate Cements: Impact of Polymer Molecular Weight on Properties

Shokoufeh Borhan[1*], Ehsan Fallah[2], Seyyed Reza Sharifzadeh[3], Mohammad Hossein Shahrezaee[4, 5], Seyed shahab Ghazi Mirsaeid[6], Sara Keshtkari[7]

1. Department of Materials, Chemical and Polymer Engineering, Buein Zahra Technical University, Buein Zahra, Iran.
2. Department of Orthopedics, School of Medicine, AJA University of Medical Sciences, Tehran, Iran.
3. Department of Orthopedic Surgery, AJA University of Medical Sciences, Tehran, Iran.
4. School of Dentistry, Tehran University of Medical Sciences, Tehran, Iran.
5. Department of Oral and Maxillofacial Surgery, TD.C., Islamic Azad University, Tehran, Iran.
6. Department of Neurosurgery, School of Medicine, AJA University of Medical Sciences, Tehran, Iran.
7. Department of Internal Medicine, School of Medicine, AJA University of Medical Sciences, Tehran, Iran.

Use your device to scan and read the article online

Citation Borhan Sh, Fallah E, Sharifzadeh SZ, Shahrezaee MH, Ghazi Mirsaeid S, Keshtkari S. Comparative Study of Chitosan/Hyaluronic Acid Modified Injectable Calcium Phosphate Cements: Impact of Polymer Molecular Weight on Properties. Journal of Translational Regenerative Medicine. 2025; 1:E1015. http://dx.doi.org/10.32598/JTRM.1.1015

http://dx.doi.org/10.32598/JTRM.1.1015

ABSTRACT

Background: Despite significant progress in calcium phosphate cement (CPC) development, conventional formulations still suffer from limitations that limit their clinical applicability.

Methods: In this study, novel injectable nanocomposite bone cements for bone and cranial defect reconstruction were developed by incorporating an equimolar mixture of tetracalcium phosphate (TTCP) and dicalcium phosphate dihydrate (DCPD) powders as the primary reactive phase into 3 wt/v% hyaluronic acid (HA) solutions with two different molecular weights (500 and 1750 kDa). The physical, physicochemical, and structural properties of the developed cements were evaluated and compared with those of conventional CPC, prepared using the same powder phase and distilled water as the liquid component.

Results: It was demonstrated that the prolonged setting time and low compressive strength of CPC can be significantly improved by incorporating HA in a molecular-weight-dependent manner. HA also acted as a viscosity-enhancing agent, showing a pronounced effect on cement injectability, particularly with high-molecular-weight HA. X-ray diffraction (XRD) analysis of the set cements revealed that, in both control and HA-containing formulations, the initial reactants were completely converted into nanostructured apatite after immersion in simulated body fluid. A slightly higher rate of apatite formation was observed in the HA 1750 kDa group compared to the other formulations. SEM observations confirmed a globular microstructure composed of tightly interconnected plate-like apatite nanocrystals in all samples.

Conclusion: The developed calcium phosphate–HA nanocomposite cements have strong potential to be used as injectable bone graft materials for bone defect repair following appropriate in vivo evaluations.

Keywords: Chitosan, Hyaluronic acid, Calcium phosphate cements (CPCs), Molecular weight

Article info:
Received: 10 Jun 2026
Accepted: 25 Jul 2026
Publish: 05 Sep 2026

*** Corresponding Author:**
Shokoufeh Borhan, Assistant Professor.
Address: *Department of Materials, Chemical and Polymer Engineering, Buein Zahra Technical University, Buein Zahra, Iran.*
Phone: *+98 (28) 33894000*
E-mail: *shkfborhan@bzte.ac.ir*

Highlights

- Despite significant progress in CPC development, conventional formulations still suffer from limitations, which limit their clinical applicability.

- In this study, injectable calcium phosphate/HA nanocomposite cements using TTCP and DCPD, combined with HA, were developed for bone and cranial defect reconstruction.

- The developed nanocomposite cements showed strong potential to be used as injectable bone graft materials for bone defect repair.

Plain Language Summary

The calcium phosphate cements (CPCs), including Hap, have been widely investigated for orthopedic and dental applications. However, their use has several limitations. To address these limitations, non-ceramic HAp systems, commonly known as HAp cements, have been developed. Natural polysaccharides, such as HA offer distinct advantages due to their hydrophilicity. In this study, injectable calcium phosphate/HA nanocomposite cements incorporating tetracalcium phosphate (TTCP) and dicalcium phosphate dihydrate (DCPD) were developed for bone and cranial defect reconstruction. The physical, physicochemical, and structural properties of the developed cements were evaluated and compared with those of conventional CPC. The prolonged setting time and low compressive strength of CPC were significantly improved by incorporating hyaluronic acid (HA). In conclusion, the incorporation of biocompatible and biodegradable polymers such as HA or chitosan into CPCs significantly improves its unfavorable properties, including long setting time and low mechanical strength. The developed nanocomposite cements have the potential to be used as injectable bone graft materials for bone defect repair.

Introduction

Calcium phosphate cements (CPCs) are a relatively new class of calcium phosphate-based biomaterials developed to overcome several limitations of monolithic calcium phosphate ceramics. These cements are typically composed of a powder phase and a liquid phase. The powder phase generally consists of one calcium phosphate compound or combined calcium phosphate compounds, while the liquid phase may include distilled water, phosphate-buffered solutions, or organic aqueous solutions. Upon mixing at an appropriate powder-to-liquid ratio, a moldable paste is formed, which subsequently hardens after a defined setting time [1-3]. The setting process of CPCs is primarily governed by precipitation reactions occurring in the paste, leading to the formation of secondary calcium phosphate phases such as brushite, octacalcium phosphate, or hydroxyapatite (HAp). The mechanical integrity of the set cement arises from the interlocking and entanglement of these precipitated crystalline phases [4]. Accordingly, CPCs can be classified by the dominant precipitated phase formed during setting, which is largely determined by the calcium/phosphorus (Ca/P) ratio and the system's physicochemical characteristics, as well as processing parameters such as particle size, pH, and liquid composition [5].

Among the various end products, HAp is of particular importance due to its close similarity to the mineral phase of natural bone [6, 7]. Consequently, it has been widely investigated for orthopedic and dental applications [8]. However, the direct use of sintered HAp ceramics is associated with several limitations, including their high crystallinity and limited bioresorbability, difficulty in shaping complex geometries that match bone defects, and the requirement for high-temperature processing conditions [9-11]. Moreover, conventional ceramic processing restricts the incorporation of biologically active molecules such as growth factors and osteoinductive proteins, which are essential for enhancing bone regeneration [12, 13]. To address these limitations, non-ceramic HAp systems, commonly known as HAp cements, have been developed. In this context, the term "non-ceramic" refers to the absence of high-temperature processing during material preparation. These cements are typically formed by mixing a calcium phosphate-based powder phase, consisting of acidic and basic calcium phosphate components, with an aqueous liquid phase [14, 15]. The setting reaction involves the in situ formation of nanocrystalline HAp or calcium-deficient HAp within the paste, resulting in a hardened structure with a bone-like composition and morphology [16-18].

In parallel with advancements in calcium phosphate systems, polymer-based biomaterials have gained increasing attention in biomedical engineering due to their tunable mechanical properties, degradation behavior, permeability, solubility, and transparency [19-21]. Natural polymers are particularly attractive because of their inherent biocompatibility and biodegradability [22, 23]. Synthetic polymers such as polylactic acid (PLA) and polyglycolic acid (PGA), along with their copolymers, have been extensively studied for applications in bone tissue engineering and drug delivery systems [24, 25]. However, a major challenge for many synthetic polymers is their limited bioactivity and suboptimal interactions with biological environments [26, 27].

Natural polysaccharides, a subclass of biopolymers, offer distinct advantages due to their hydrophilicity, structural diversity, and ease of processing [28]. These macromolecules, including alginate, chitosan, agarose, starch, and cellulose derivatives, have been widely used as scaffolding and cell-supporting matrices in tissue engineering [29, 30]. Their structural variability, arising from different monosaccharide units and glycosidic linkages, enables the design of materials with tailored biological and mechanical properties [31]. Among polysaccharides, hyaluronic acid (HA) is a particularly important glycosaminoglycan widely distributed in the extracellular matrix of vertebrate tissues [32, 33]. HA plays a crucial role in tissue hydration, lubrication, and cell signaling, and is abundant in biological fluids such as synovial fluid and vitreous humor [34]. Structurally, it is composed of repeating disaccharide units of D-glucuronic acid and N-acetyl-D-glucosamine linked via β(1→3) and β(1→4) glycosidic bonds [35]. Unlike other glycosaminoglycans, HA is non-sulfated, which contributes to its unique physicochemical and biological properties [36].

One of the most notable characteristics of HA is its exceptional hydrophilicity and high viscosity, even at low concentrations. In aqueous environments, HA chains adopt extended conformations stabilized by intramolecular hydrogen bonding and interactions with water molecules, forming highly hydrated networks. This property enables HA to act as a natural lubricant, reducing friction between biological tissues, particularly in synovial joints [37, 38]. Clinically, HA-based formulations are widely used in the treatment of osteoarthritis to restore synovial fluid viscosity and improve joint mobility [39]. In addition to its rheological properties, HA plays an important role in cell proliferation, migration, and tissue regeneration [40]. It is biodegradable in vivo via hyaluronidase-mediated enzymatic degradation, producing oligosaccharides and low-molecular-weight fragments, some of which exhibit pro-angiogenic activity [41]. Owing to its excellent biocompatibility, non-immunogenicity, and functional versatility, HA has been widely used in drug delivery systems, wound healing, and tissue-engineering scaffolds [42, 43]. From a biomaterials perspective, HA is particularly attractive as a modifying agent for CPCs due to its ability to regulate viscosity, influence ion interactions, and provide biologically relevant functional groups such as carboxyl and hydroxyl moieties. These functional groups can interact with calcium ions and serve as nucleation sites for apatite formation, potentially influencing both the kinetics of cement setting and the microstructure of the final mineral phase [44].

Despite significant progress in CPC development, conventional formulations still suffer from limitations, including prolonged setting time, insufficient mechanical strength, and poor injectability, which limit their clinical applicability, particularly in minimally invasive surgical procedures [45]. Therefore, the incorporation of biologically active and structurally functional polymers such as HA offers a promising strategy to simultaneously enhance handling properties and biological performance. In this context, the present study focuses on the development of injectable calcium phosphate/HA nanocomposite cements using tetracalcium phosphate (TTCP) and dicalcium phosphate dihydrate (DCPD), as reactive phases, combined with HA solutions of different molecular weights. The study aims to evaluate the effect of HA on setting behavior, mechanical performance, injectability, microstructure, apatite formation, and biological response. By integrating a bioactive polymer naturally present in the extracellular matrix, this study seeks to bridge the gap between conventional CPCs and the hierarchical structure of natural bone, thereby advancing the design of next-generation bone-substitute materials.

Materials and Methods

Preparation of CPC powders

The CPCs based on TTCP and DCPD were developed in this study. The TTCP powder was synthesized according to a conventional solid-state reaction method. Briefly, equimolar amounts of calcium carbonate ($CaCO_3$; Merck, Germany) and dicalcium phosphate anhydrous ($CaHPO_4$; Merck, Germany) were mixed and homogenized in a planetary ball mill for 1 h. The homogenized mixture was transferred into an alumina crucible and heat-treated at 1500 ˚C for 6 h in an electric furnace. After thermal treatment, the samples were rapidly quenched to room temperature in a desiccator to preserve the desired phase composition. The obtained clinker was crushed

and subsequently milled in a planetary ball mill for 30 minutes to obtain TTCP powder with a mean particle size of approximately 13 μm. The cement powder phase was prepared by mixing TTCP (Dmean=13 μm) and DCPD (Dmean=5 μm) at an equimolar ratio. Powder blending was carried out in a planetary ball mill using polyethylene containers and alumina milling balls for 30 min to ensure homogeneous mixing and adequate particle activation.

Preparation of liquid phases

Four different liquid phases were employed for cement preparation. Distilled water was used to prepare the control CPC. A 3 wt/v% chitosan solution prepared in acetic acid (Merck, Germany) was used for the CFC–chitosan composite. Chitosan powder was supplied by Chitotech Company, Iran. In addition, two 3 wt/v% HA solutions with molecular weights of 500 kDa (Shaanxi Sciphar Biotechnology, China) and 1750 kDa (Jinan Haohua Industry, China) were prepared in 0.5 M acetic acid and used to fabricate the CPC500 and CPC1750 formulations.

Cement preparation and simulated body fluid (SBF) immersion

The powder-to-liquid (P/L) ratio for each formulation was optimized to achieve homogeneous and workable cement pastes. The P/L ratio for the control CPC was 3.5 g/mL, while values were 3.3, 3.1, and 2.8 g/mL for CPC500, CPC1750, and CPC-CH formulations, respectively. After mixing, the cement pastes were transferred into molds and allowed to set at 37 ˚C under 100% relative humidity for 24 h in an incubator (EHRET KBK4200). The set specimens were subsequently immersed in SBF for up to 21 days to evaluate their in vitro bioactivity and structural stability.

X-ray diffraction (XRD) analysis

The phase composition of the set cements before and after immersion in SBF was analyzed by XRD. After 24 h of setting or after removal from SBF solution, the specimens were thoroughly washed with distilled water, dried, and ground into fine powders. The XRD analysis was performed using a Philips PW 3710 diffractometer equipped with Cu-Kα radiation (λ=1.54 Å) and a Ni filter. Measurements were conducted at 40 kV and 30 mA over a 2θ range of 20–50˚.

Fourier transform infrared spectroscopy (FTIR)

FTIR was used to investigate the functional groups and apatite formation in the cement structures before and after immersion in SBF. Approximately 2 mg of the powdered sample was mixed with 800 mg KBr and compressed into transparent pellets. FTIR spectra were recorded using a BRUKER VECTOR 33 spectrometer within the range of 400–4000 cm^{-1} at a resolution of 2 cm^{-1}.

Microstructural characterization

The microstructure of the set and SBF-immersed cement samples was examined using scanning electron microscopy (SEM) equipped with energy-dispersive X-ray analysis (EDX) (StereoScan S360 Cambridge). Disc-shaped specimens with a diameter of 10 mm and a thickness of 5 mm were used for analysis. Prior to SEM analysis, the samples were coated with a thin gold layer to improve electrical conductivity.

Initial setting time measurement

Initial setting time was measured using a Gillmore needle apparatus in accordance with the ASTM C266-89 standard. The setting time was defined as the interval between the start of mixing and the time at which a Gillmore needle weighing 113.4 g with a tip diameter of 2.13 mm failed to produce a visible indentation on the cement surface. For each measurement, the cement paste was placed into a mold and tested 3 minutes after mixing. The needle was carefully lowered vertically onto the cement surface for 5 seconds at 10-second intervals until no penetration was observed. Four specimens from each composition were evaluated, and the average value was reported.

Compressive strength test

Compressive strength was measured in accordance with ANSI/ADA Specification No. 30/2001. Cement pastes were poured into cylindrical Teflon molds with a diameter of 6 mm and a height of 12 mm. After complete setting, the specimens were removed from the molds and stored at 37 ˚C and 100% humidity for 24 h. Mechanical testing was performed using a universal testing machine (Zwick/Roell-HCR 25/400) at a crosshead speed of 1 mm/min. Four specimens were tested for each cement formulation.

Injectability evaluation

Injectability of the cement pastes was evaluated using a universal testing machine (Zwick/Roell-HCR 25/400) at a crosshead speed of 5 mm/min. Cement pastes were loaded into 10 mL syringes equipped with a nozzle diameter of 800 μm. A compressive force was applied vertically to the syringe plunger, and force–displacement curves were recorded for all formulations.

In vitro biocompatibility assessment

Biocompatibility of the prepared cements was evaluated using osteoblast cells isolated from neonatal rat calvaria. Cells were cultured in Dulbecco's modified Eagle medium (DMEM) supplemented with 15% fetal bovine serum (FBS) and penicillin under a humidified atmosphere containing 95% air and 5% CO_2. Cell viability and proliferation on the cement surfaces were assessed using the MTT assay. Cement discs were sterilized with 70% ethanol before cell seeding. Osteoblast cells were seeded onto the sample surfaces at a density of 1×10^4 cells per sample and incubated for 1, 7, and 14 days at 37 ˚C under 100% humidity and 5% CO_2 atmosphere. The culture medium was refreshed every three days. Cell morphology and attachment on the cement surfaces after 1 and 7 days of culture were evaluated by SEM following standard fixation procedures described in previous studies.

Results

XRD analysis

The XRD patterns of the control CPC, CPC-CH, CPC500, and CPC1750 after 24 h of incubation and after 1, 3, and 7 days of immersion in SBF solution are shown in Figure 1. The diffraction pattern of the initial cement powder is also included for comparison. In all cement formulations, the apatite phase, the main product of the setting reaction, was detected after setting (24 h incubation), along with the remaining TTCP and DCPD precursor phases. Upon immersion in simulated body fluid (SBF) solution, the intensities of the TTCP and DCPD peaks gradually decreased, while the intensity of the apatite peaks increased significantly. The progressive conversion of the initial reactant phases into HAp with increasing immersion time was clearly observed. After 7

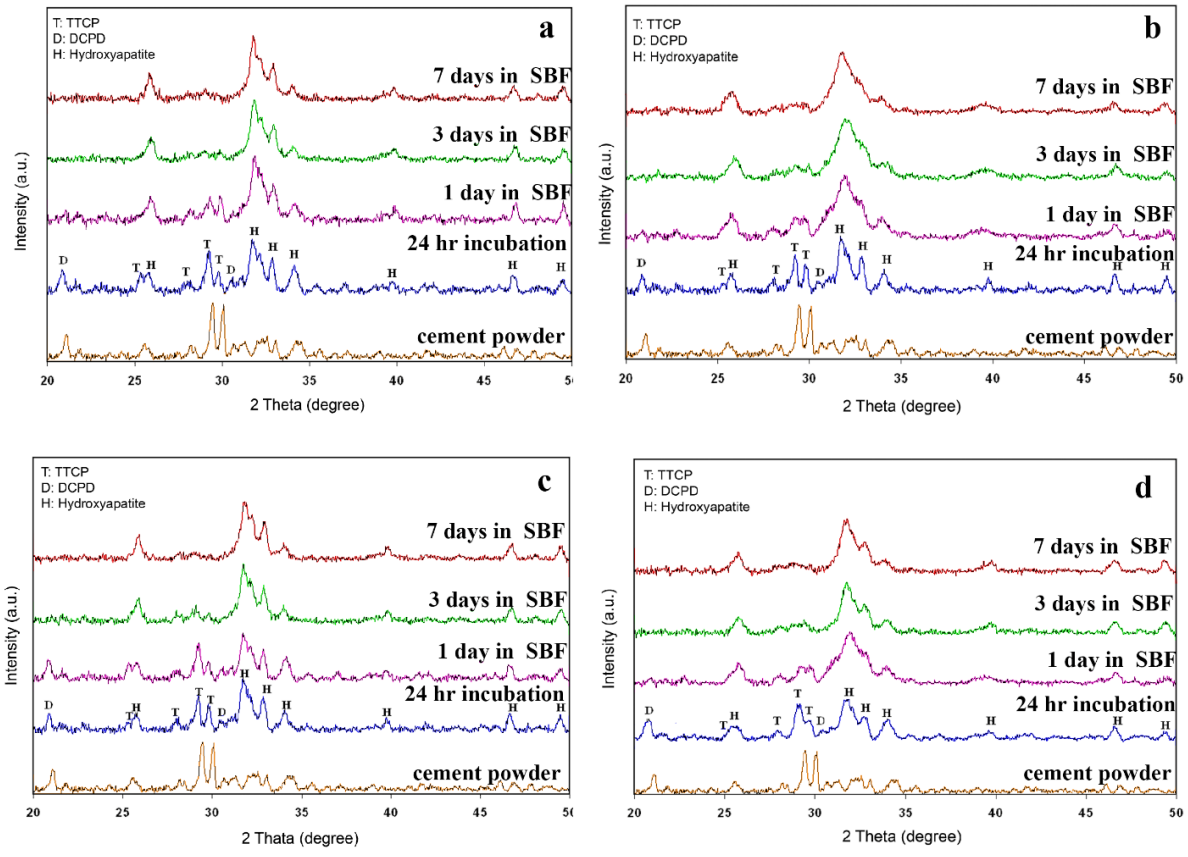

Figure 1. The XRD patterns of (a) control CPC, (b) CPC-CH composite, (c) CPC500 composite, and (d) CPC1750 composite

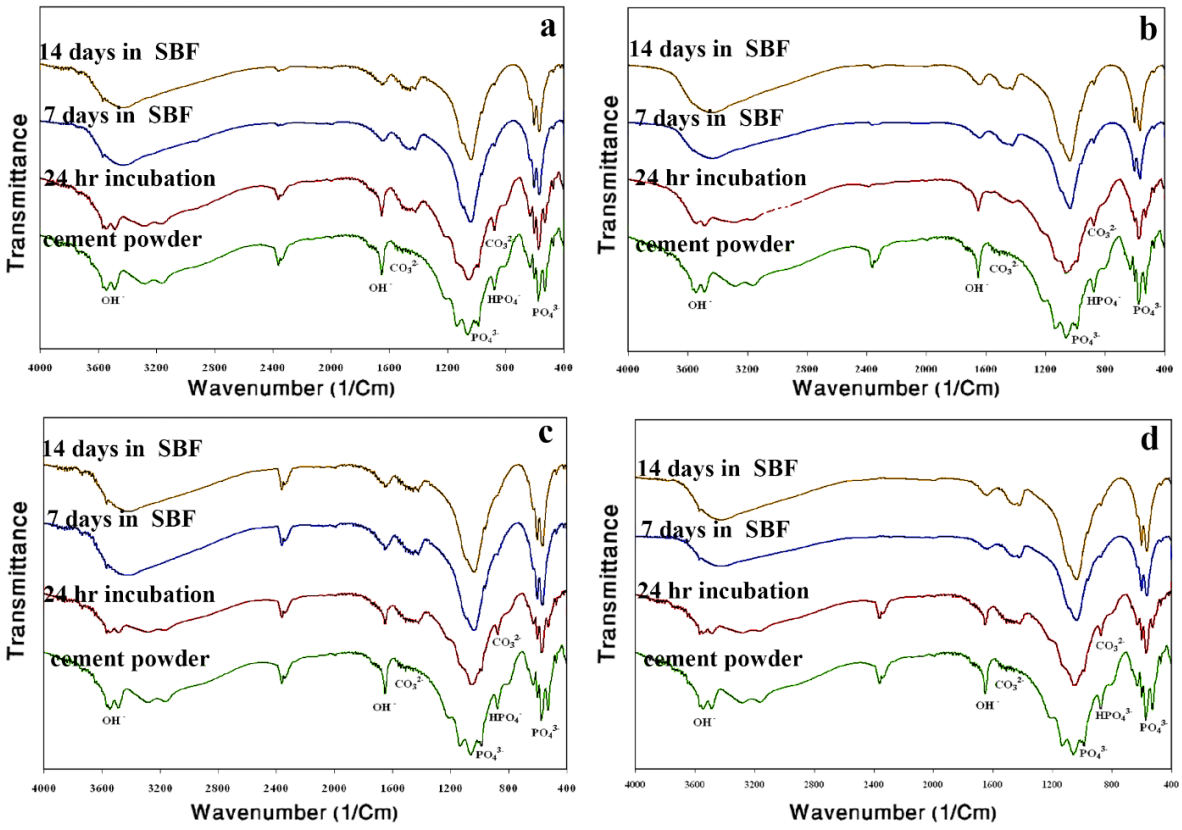

Figure 2. FTIR spectra of (a) control CPC (b) CPC-CH composite, (c) CPC500 composite, and (d) CPC1750 composite.

days of immersion, the diffraction peaks corresponding to the reactant phases almost completely disappeared, and apatite became the dominant phase in all cement samples.

The XRD patterns of the control and composite cements after 14 and 21 days of immersion were similar to those obtained after 7 days; therefore, these patterns were not presented to avoid repetition. The incorporation of chitosan into the composite cement formulation did not noticeably delay apatite formation. However, the CPC1750 sample appeared to exhibit a slightly faster apatite formation rate compared to other formulations, as the intensities of the TTCP and DCPD peaks after 1 day of immersion were lower than those observed for the other cements. Nevertheless, after 3 days of immersion in SBF, most of the reactant phases were consumed across all formulations, and apatite became the predominant phase.

These findings indicate that the addition of chitosan and HA does not significantly affect the nature of the final reaction product. However, increasing the molecular weight of HA, as in the CPC1750 formulation, slightly accelerates apatite formation. Furthermore, the broad diffraction peaks observed in the XRD patterns suggest low crystallinity and a nanoscale crystal size in the formed apatite phase.

FTIR analysis and identification of functional groups in cement compositions

FTIR spectroscopy was performed for all cement formulations, including control CPC, CPC-CH, CPC500, and CPC1750. The analyses were carried out after 24 h of incubation at 37 ˚C and also after 7 and 14 days of immersion in SBF solution. Figure 2 presents the FTIR spectra of the control and experimental cements. The FTIR spectrum of the initial cement powder is also included in the figure for comparison.

The absorption bands observed at approximately 545, 565, and 1070 cm^{-1} correspond to phosphate groups and were detected in all samples. The peak located at around 1448 cm^{-1} is attributed to carbonate groups. In the hardened cement samples after 24 h of incubation, this peak mainly originated from the presence of calcium carbonate, while in the SBF-immersed samples, it was associated with carbonate incorporation into the HAp structure. In addition, a shoulder observed near 870 cm^{-1}

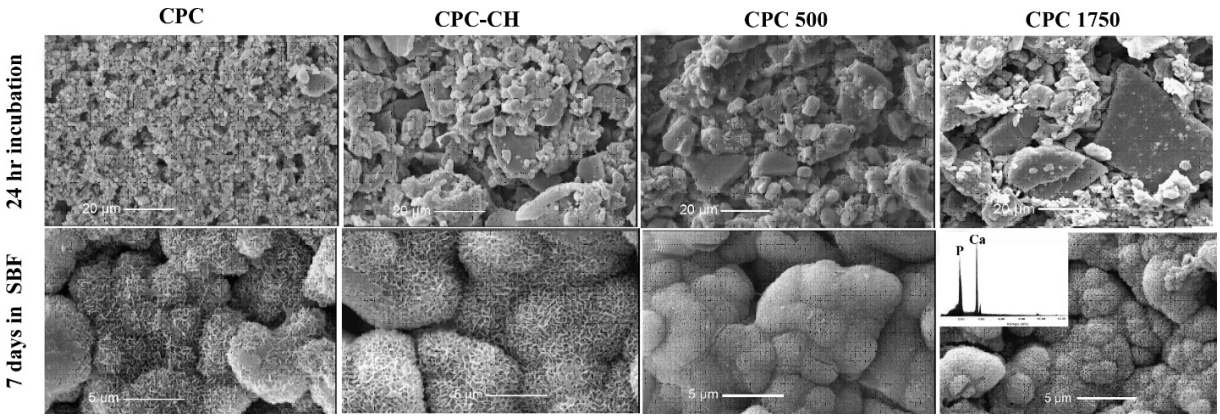

Figure 3. Microstructure of different cements after 24 h incubation and after 7 days immersion in SBF

corresponds to carbonate-substituted apatite, confirming the formation of carbonated HAp in the cement matrix.

Furthermore, the carbonate-related CO_3^{2-} absorption band, which appeared as a single peak in the incubated samples, gradually split into two distinct peaks after immersion in SBF solution. A shoulder near 870 cm^{-1} was also observed in all immersed samples. These spectral changes indicate the substitution of carbonate ions for phosphate groups within the apatite lattice. Since carbonate ions are abundantly present in SBF solution, they can readily penetrate the HAp structure during the mineralization process.

The formation of hydroxylated apatite after immersion in SBF was further confirmed by the appearance of the OH^- absorption band near 3550 cm^{-1}, which is characteristic of HAp. No significant differences were observed between the FTIR spectra of the control and experimental cements, indicating that the addition of chitosan and HA did not substantially alter the chemical structure of the final apatite phase. The FTIR spectra of samples immersed in SBF for 21 days were similar to those obtained after 14 days of immersion; therefore, these spectra are not presented to avoid repetition.

Microstructure and morphology of the cements

The microstructure of CPC, CPC-CH, CPC500, and CPC1750 after 24 h of setting and incubation at 37 ˚C is shown in Figure 3. In the CPC sample, the microstructure consisted of calcium phosphate particles exhibiting two distinct morphologies: coarse particles ranging from 1 to 5 µm and finer particles smaller than 1 µm, which were located either on the surfaces of larger particles or within interparticle spaces. In addition, micro-porosities smaller than 5 µm were observed within the structure, which can be attributed to the removal of the liquid phase during cement setting. Very fine needle-like crystals were also present between the reactive particles or on their surfaces, which are likely associated with precipitated apatite phases. The microstructure and morphology of calcium phosphate particles in the composite cements differ significantly from those of control CPC. In these cements, the reactive particles appear to be coated and interconnected by a viscous phase. In these samples, the particle surfaces were smoother compared to the control CPC, and small surface pores were observed, which are likely related to entrapped air bubbles.

After 7 days of immersion in SBF solution, a globular microstructure composed of tightly intergrown nanocrystals was observed in all cement samples (Figure 3). This morphology is characteristic of HAp formed via a dissolution–precipitation mechanism on the cement surface.

It seems that the morphology of the precipitated crystals varies among the samples. CPC and CPC-CH exhibit predominantly plate-like crystal morphologies, whereas in HA-containing composites, the crystals have bending-twisting rod-like structures, with smaller crystal sizes compared to the control CPC. SEM analysis revealed that the apatite crystal size was approximately 100 nm in control CPC, while it was reduced to about 30–50 nm in the composites.

According to the EDXA pattern of the CPC1750 after 7 days of immersion in SBF (Figure 3), only phosphorus and calcium were detected, confirming that the formed crystals are calcium phosphate.

Setting time, mechanical strength, and injectability

Figure 4 compares the initial setting time of CPCs and the compressive strength of different cement formulations after 24 h incubation at 37 ˚C under 100% humid-

ity. The presence of chitosan in the cement structure led to a slight increase in mechanical strength and a moderate reduction in setting time. With the incorporation of HA, the setting time decreased significantly, from approximately 90 min for control CPC to about 20–30 min for HA-containing cements. The difference in setting time between CPC500 and CPC1750 samples was not statistically significant. In addition, the presence of HA resulted in a significant increase in compressive strength ($P< 0.05$). The molecular weight of HA also directly influenced the enhancement of mechanical properties. It is evident that the initial setting of apatite-forming CPCs is primarily governed by the interlocking of precipitated apatite crystals within the cement paste. However, it should be noted that the setting behavior of a cement with a fixed composition also depends on factors such as particle size, environmental pH, powder-to-liquid ratio, and other parameters.

There was also a direct relationship between the amount of HAp formed in the cement and its mechanical strength. Any factor that accelerates HAp formation tends to enhance the mechanical strength of the cement [46]. In addition to the ratio of reactive components, other parameters such as particle size of reactants, differences in Ca and P ion diffusion rates, diffusion distance through the HAp layer formed on particle surfaces, crystal size of apatite, powder-to-liquid ratio, and porosity are all factors that can influence the mechanical properties of the cement. The relatively low compressive strength of CPCs is mainly attributed to weak bonding between apatite crystals and to a high degree of microporosity within their structure.

Chitosan is soluble only in acidic solutions, whereas it becomes insoluble under alkaline conditions. Mixing a chitosan solution with CPC powder raises the pH, thereby transforming the soft CPC-CH paste into an elastomeric solid. Therefore, the initial setting of this composite is governed not only by the slow conversion of TTCP and DCPD into HAp but also by the presence of chitosan, which elevates pH and reduces setting time [47].

As previously discussed, in the control CPC, strength is mainly provided by the interlocking of apatite crystals. However, in the CPC-CH composite, in addition to this mechanism, the presence of chitosan also promotes bonding between particles and newly formed crystals, which may explain the improved mechanical strength of the composite cement. Apatite crystals precipitate on calcium phosphate reactant particles, and their interwoven structure provides mechanical support. In the presence of HA, interactions between carboxylic groups of HA and calcium ions on the surface of TTCP and DCPD particles lead to enhanced mechanical strength. With increasing molecular weight of HA, the number of COOH groups and potential interaction sites increases, resulting in higher mechanical strength. Furthermore, the formation of calcium carboxylate complexes and their precipitation within the system contributes to a reduction in setting time, and the concentration of these complexes increases with HA molecular weight.

In addition, HA acidifies the cement liquid phase, thereby bringing the solution into a supersaturated state with respect to HAp. This accelerates the dissolution of TTCP and DCPD, thereby increasing the rate of setting reaction and reducing the setting time [48]. COOH groups also act as favorable nucleation sites for apatite crystal formation [49]. Consequently, in HA-containing cements, increasing HA molecular weight enhances the conversion rate of reactants into apatite crystals, which is also supported by XRD results.

Figure 4c clearly illustrates the differences in injectability behavior among all cement formulations. The clinical application of conventional CPCs in orthopedic and spinal surgeries is limited due to poor injectability and structural disintegration upon exposure to physiological fluids. Phase separation of solid and liquid components, known as filter pressing, is a common issue affecting cement injectability [50]. The presence of even small amounts of dispersed particles during surgery may cause severe inflammatory responses, vascular obstruction, and pulmonary embolism [51]. A novel approach to bone tissue regeneration involves developing injectable, shapeable cement systems that can be delivered directly to the defect site. This strategy has gained significant attention in minimally invasive orthopedic surgeries. Such systems reduce surgical time, minimize the risk of infection, reduce damage to surrounding muscle tissue, and can also contribute to lower overall treatment costs.

In the control CPC, injectability from point A1 to A2 occurs smoothly under an approximately constant force. Point A2 marks the onset of phase separation (filter pressing), where from A2 to A3, a portion of the paste is extruded with a higher liquid fraction, while the solid phase remains inside the syringe. Consequently, a higher force is required to extrude the remaining paste. Beyond point A3, further increases in force do not enhance paste extrusion due to intensified phase separation between the liquid and powder phases; instead, the applied force causes the syringe plunger to bend, a phenomenon also observed experimentally. In this sample, approximately

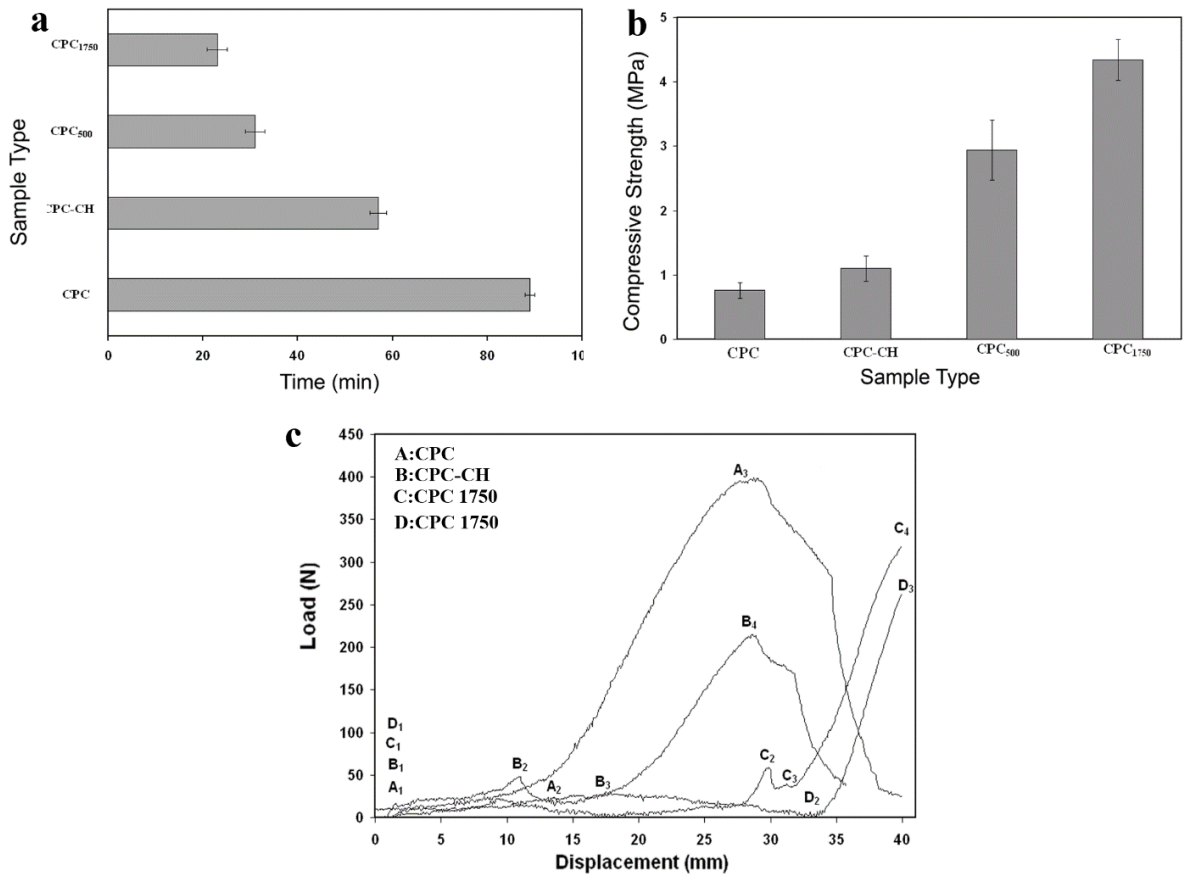

Figure 4. Initial setting time (a), compressive strength (b), and typical force–displacement curves from injectability tests of different CPCs (c)

32% of the material volume was successfully injected, with injection ending at 40 mL.

In the CPC-CH sample, injection from point B1 to B3 occurs easily with a force below 20 Newton (N). A slight increase in force at point B2 is likely attributed to air release from the paste. The region from B3 to B4 corresponds to paste extrusion accompanied by an increase in force, where filter pressing also occurs. Beyond B4, as in the control sample, a further increase in force is ineffective due to severe phase separation, and the remaining paste cannot be extruded, resulting in the syringe plunger bending. Nevertheless, approximately 50% of the paste volume was successfully injected, which is about 20% higher than that of the control CPC. Additionally, phase separation in this sample was less pronounced than in the control cement. Chitosan acts as a viscosity-enhancing agent, improving water retention within the cement paste and reducing the likelihood of particle disintegration [52]. In addition to increasing viscosity, chitosan can chelate calcium ions and act as a binding agent, enhancing cohesion between cement particles [53], thereby improving injectability.

In HA-containing samples, more than 85% of the paste volume can be easily injected with a force below 10 N. The remaining paste (point C3 in CPC500 and point D2 in CPC1750) is extruded with increasing force, and at points C4 and D3, the syringes are completely emptied. It should be noted that at all stages of injection, the required force for CPC1750 is lower than that for CPC500. The peak force observed at point C2 is attributed to the expulsion of air bubbles from the cement paste. The HA in CPC composites also has water retention capability and, similar to chitosan, reduces particle disintegration. The improved injectability of CPC in the presence of HA is mainly due to increased viscosity of the liquid phase and stronger interparticle interactions, which are more pronounced than those observed with chitosan. This viscous layer between particles provides a lubricating medium that facilitates particle sliding during injection and prevents the phase separation commonly observed in conventional CPC pastes. Increasing the molecular

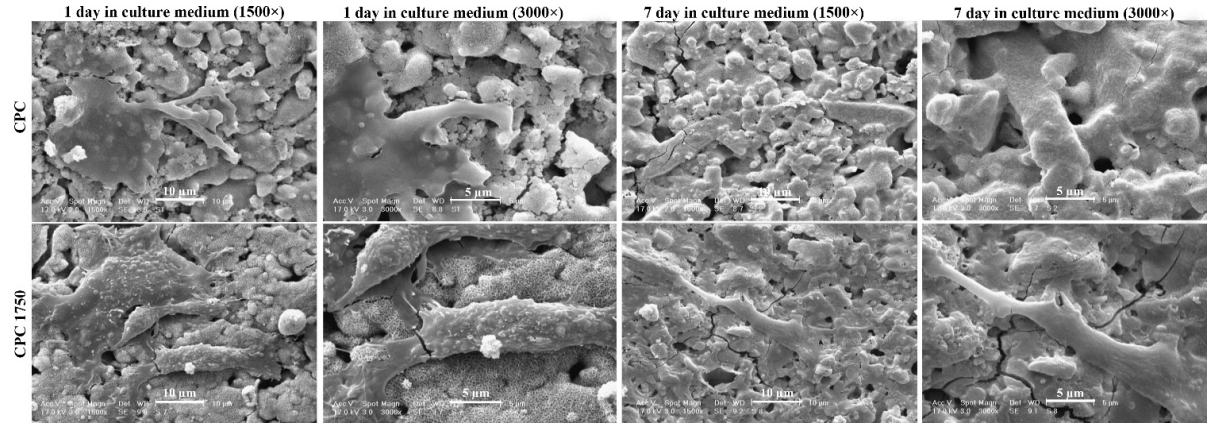

Figure 5. SEM images at different magnifications showing CPC and CPC1750 samples' surfaces with cells after 1 and 7 days of culture in medium

weight of HA further enhances liquid-phase viscosity, thereby improving injectability.

Cell morphology

Figure 5 presents the SEM images of the control CPC and CPC1750 composite samples after 1 and 7 days of cell culture at different magnifications. The micrographs revealed the morphology of osteoblastic cells on the surface of the samples. The cells exhibited a well-spread morphology and adhered to the substrate through interactions with needle-like apatite crystals. Cell adhesion appears to be facilitated by the rough surface topography, which promotes the interlocking of cellular protrusions. The flattened morphology of the cells indicates their strong affinity for the surface, confirming the good biocompatibility of both cement samples. The small spherical features observed on the cell surface in the CPC1750 sample are due to cellular secretions, suggesting enhanced enzymatic and metabolic activity of cells in the HA-containing composite.

After 7 days, the cell layers gradually reach a confluent state, where adjacent cells form continuous interconnected networks. As previously discussed, the precipitation of apatite crystals during hydrolysis and related reactions also contributes to cell attachment and morphological development. In fact, during the 7-day culture period, simultaneous cell proliferation and apatite deposition occur, leading to partial coverage of cells by apatite layers. This phenomenon is less pronounced in HA-containing samples, where more uniform cell confluence was observed.

Discussion

The present study demonstrated that modifications in CPC composition through incorporation of chitosan and HA significantly influence the physicochemical behavior, microstructure, and biological performance of the system. Overall, the results highlight that the evolution of HAp is the dominant process governing setting, mechanical development, and bioactivity, while the added biopolymers mainly act as modulators of kinetics, ion interaction, and interfacial properties.

The formation of carbonated and poorly crystalline HAp suggests that the cement system follows a dissolution–precipitation pathway typical of apatite-forming calcium phosphate materials. This dissolution–precipitation mechanism is considered the fundamental setting process in CPCs, where calcium and phosphate ions released from precursor phases subsequently reorganize into poorly crystalline apatite structures [54]. The presence of organic additives does not alter the final chemical identity of the mineral phase but may influence crystal growth dynamics and nucleation density. This is reflected in the formation of nanoscale apatite crystals with varying morphology, indicating that the organic environment affects crystal habit rather than phase composition.

Microstructural observations indicate that the incorporation of chitosan and HA introduces a viscous organic phase that modifies particle interactions and improves cohesion within the cement paste. This results in a more continuous matrix with reduced interparticle voids compared to the control formulation. Such microstructural rearrangement is important because mechanical integrity in CPCs is largely governed by particle interlocking and the degree of porosity within the hardened structure.

The enhancement in mechanical properties can be attributed to synergistic interactions between newly formed apatite crystals and polymeric chains. In particular, functional groups such as amino groups in chitosan and carboxyl groups in HA can interact with calcium ions on particle surfaces, promoting interfacial bonding and reinforcing the developing structure. These interactions likely improve load transfer between particles and reduce microstructural defects that typically weaken CPCs [55].

The observed reduction in setting time in polymer-containing systems can be explained by accelerated dissolution–precipitation kinetics. Acidic or functional group-rich environments can increase local ion availability and promote supersaturation with respect to apatite, thereby enhancing nucleation rates. Additionally, polymer-induced changes in viscosity and ion diffusion pathways may facilitate more rapid structural organization of the setting cement.

Improvements in injectability are closely related to the rheological modifications introduced by both polymers. The presence of a viscous liquid phase reduces particle–particle friction and prevents phase separation during extrusion. This ensures more homogeneous paste flow and minimizes filter-pressing phenomena commonly observed in conventional calcium phosphate systems. The stronger effect observed for HA-containing formulations suggests that molecular weight and chain entanglement significantly influence flow behavior and paste cohesion.

From a biological perspective, the improved cellular response observed on composite surfaces can be linked to both chemical and physical surface modifications. The presence of nanoscale apatite crystals enhances surface roughness and provides favorable sites for protein adsorption and cell anchorage. In addition, polymer-modified surfaces may facilitate more stable cell adhesion by improving hydration layers and surface bioactivity. The formation of continuous cell layers over time further confirms the cytocompatibility of the developed materials and suggests their suitability for supporting osteoblastic activity [56].

Interestingly, the reduced interference of apatite deposition on cell spreading in polymer-containing samples indicates a more controlled mineralization environment, which may better support cell proliferation and uniform tissue formation. This balance between mineral formation and cellular activity is critical for successful bone regeneration applications.

Overall, the findings indicate that while HAp formation governs the fundamental bioactivity of the system, incorporating chitosan and HA provides an effective strategy to tailor mechanical performance, injectability, and biological response without altering the final apatite phase. This combination of effects makes the developed system a promising candidate for injectable bone repair applications where both handling properties and biological performance are essential.

Conclusion

● Based on the experimental results and the obtained findings, the following conclusions can be drawn:

● The incorporation of biocompatible and biodegradable polymers such as HA or chitosan into CPCs significantly improves its unfavorable properties, including long setting time and low mechanical strength.

● HA exhibits a more pronounced effect than chitosan in enhancing the physical, physicochemical, and structural properties of CPC.

● The molecular weight of HA is an important parameter influencing the modification of cement properties, such that composites prepared with higher molecular weight HA demonstrate improved structural performance.

● In HA-containing CPC composites with higher molecular weight, the setting time is significantly reduced, while mechanical strength is considerably increased.

● The incorporation of HA markedly improves the injectability of CPCs, thereby expanding its potential use as a bone filler in minimally invasive surgical procedures, particularly in anatomically difficult-to-access regions such as the spine, ribs, and vertebrae.

● The presence of HA in the CPC formulation does not alter the type or quantity of the apatite phase formed; however, it enhances the rate of HAp formation during the setting process.

● The HAP, formed in this study as the setting product of the HA/CPC composite, exhibits a nanoscale microstructure that closely resembles the mineral phase of natural bone.

● The favorable adhesion of osteoblastic cells to the CPC surface confirms the good biocompatibility of the developed material.

● HA, similar to collagen, is a major component of the extracellular matrix and plays a key role in cell proliferation and growth. Therefore, due to the compositional similarity to natural bone, the developed CPC composites demonstrate superior performance compared to conventional single-phase calcium phosphate bone fillers.

Ethical Considerations

Compliance with ethical guidelines

There were no ethical considerations to be considered in this research.

Funding

This research did not receive any grant from funding agencies in the public, commercial, or non-profit sectors.

Authors' contributions

Conceptualization, methodology, investigation and writing: Shokoufeh Borhan; Validation and formal analysis: Ehsan Fallah; Resources: Seyyed Reza Sharifzadeh and Seyed shah Mohammad Hossein Shahrezaee; Data curation: Seyyed Reza Sharifzadeh; Supervision: Seyed shah Mohammad Hossein Shahrezaee; Project administration: Seyed shahab Ghazi Mirsaeid; Funding acquisition: Sara Keshtkari.

Conflict of interest

The authors declared no conflict of interest.

References

[1] Ambard AJ, Mueninghoff L. Calcium phosphate cement: Review of mechanical and biological properties. Journal of Prosthodontics. 2006; 15(5):321-8. [DOI:10.1111/j.1532-849X.2006.00129.x] [PMID]

[2] Takagi S, Chow LC, Hirayama S, Sugawara A. Premixed calcium-phosphate cement pastes. Journal of Biomedical Materials Research. Part B, Applied Biomaterials. 2003; 67(2):689-96. [DOI:10.1002/jbm.b.10065] [PMID]

[3] Bajammal SS, Zlowodzki M, Lelwica A, Tornetta P 3rd, Einhorn TA, Buckley R, et al. The use of calcium phosphate bone cement in fracture treatment. A meta-analysis of randomized trials. The Journal of Bone and Joint Surgery. American Volume. 2008; 90(6):1186-96. [DOI:10.2106/JBJS.G.00241] [PMID]

[4] Heinz O, Heinz H. Cement interfaces: Current understanding, challenges, and opportunities. Langmuir. 2021; 37(21):6347-56. [DOI:10.1021/acs.langmuir.1c00617] [PMID]

[5] Sun L, Chow LC, Frukhtbeyn SA, Bonevich JE. Preparation and properties of nanoparticles of calcium phosphates with various Ca/P ratios. Journal of Research of the National Institute of Standards and Technology. 2010; 115(4):243-55. [DOI:10.6028/jres.115.018] [PMID]

[6] Mohd Pu'ad NAS, Koshy P, Abdullah HZ, Idris MI, Lee TC. Syntheses of hydroxyapatite from natural sources. Heliyon. 2019; 5(5):e01588. [DOI:10.1016/j.heliyon.2019.e01588] [PMID] [PMCID]

[7] Akram M, Ahmed R, Shakir I, Ibrahim WA, Hussain R. Extracting hydroxyapatite and its precursors from natural resources. Journal of Materials Science. 2014; 49(4):1461-75. [DOI:10.1007/s10853-013-7864-x]

[8] Bordea IR, Candrea S, Alexescu GT, Bran S, Băciuț M, Băciuț G, et al. Nano-hydroxyapatite use in dentistry: A systematic review. Drug Metabolism Reviews. 2020; 52(2):319-32. [DOI:10.1080/03602532.2020.1758713] [PMID]

[9] Trzaskowska M, Vivcharenko V, Przekora A. The impact of hydroxyapatite sintering temperature on its microstructural, mechanical, and biological properties. International Journal of Molecular Sciences. 2023; 24(6):5083. [DOI:10.3390/ijms24065083] [PMID] [PMCID]

[10] Vijayan A, Vishnu J, AR, Shankar B, Sambhudevan S. A review on hydroxyapatite fabrication: From powders to additive manufactured scaffolds. Biomaterials Science. 2025; 13(4):913-45. [DOI:10.1039/D4BM00972J] [PMID]

[11] Fiume E, Magnaterra G, Rahdar A, Verné E, Baino F. Hydroxyapatite for biomedical applications: A short overview. Ceramics. 2021; 4(4):542-63. [DOI:10.3390/ceramics4040039]

[12] Lee KY, Park M, Kim HM, Lim YJ, Chun HJ, Kim H, et al. Ceramic bioactivity: Progresses, challenges and perspectives. Biomedical Materials. 2006; 1(2):R31-7. [DOI:10.1088/1748-6041/1/2/R01] [PMID]

[13] Tang Z, Li X, Tan Y, Fan H, Zhang X. The material and biological characteristics of osteoinductive calcium phosphate ceramics. Regenerative Biomaterials. 2018; 5(1):43-59. [DOI:10.1093/rb/rbx024] [PMID] [PMCID]

[14] Şahin E. Calcium phosphate bone cements. Cement based materials. InTech; 2018. [DOI:10.5772/intechopen.74607]

[15] Sugawara A, Asaoka K, Ding SJ. Calcium phosphate-based cements: Clinical needs and recent progress. Journal of Materials Chemistry B. 2013; 1(8):1081-9. [DOI:10.1039/C2TB00061J] [PMID]

[16] Zhao R, Meng X, Pan Z, Li Y, Qian H, Yang X, et al. Recent Advances in Nanohydroxyapatite: Synthesis Methods, Biomedical Applications, and Innovations in Composites. Recent Advances in Nanohydroxyapatite: Synthesis Methods. Biomedical Applications, and Innovations in Composites. 2024. [Link]

[17] Zhao R, Meng X, Pan Z, Li Y, Qian H, Zhu X, et al. Advancements in nanohydroxyapatite: Synthesis, biomedical applications and composite developments. Regenerative Biomaterials. 2025; 12:rbae129. [DOI:10.1093/rb/rbae129] [PMID] [PMCID]

[18] Wang B, Zhang Z, Pan H. Bone apatite nanocrystal: Crystalline structure, chemical composition, and architecture. Biomimetics. 2023; 8(1):90. [DOI:10.3390/biomimetics8010090] [PMID] [PMCID]

[19] Oleksy M, Dynarowicz K, Aebisher D. Advances in biodegradable polymers and biomaterials for medical applications-A review. Molecules. 2023; 28(17):6213. [DOI:10.3390/molecules28176213] [PMID] [PMCID]

[20] Kurowiak J, Klekiel T, Będziński R. Biodegradable polymers in biomedical applications: a review-developments, perspectives and future challenges. International Journal of Molecular Sciences. 2023; 24(23):16952. [DOI:10.3390/ijms242316952] [PMID] [PMCID]

[21] Kalirajan C, Dukle A, Nathanael AJ, Oh TH, Manivasagam G. A critical review on polymeric biomaterials for biomedical applications. Polymers. 2021; 13(17):3015. [DOI:10.3390/polym13173015] [PMID] [PMCID]

[22] Arif U, Haider S, Haider A, Khan N, Alghyamah AA, Jamila N, et al. Biocompatible polymers and their potential biomedical applications: A review. Current Pharmaceutical Design. 2019; 25(34):3608-19. [DOI:10.2174/1381612825999191011105148] [PMID]

[23] Asti A, Gioglio L. Natural and synthetic biodegradable polymers: Different scaffolds for cell expansion and tissue formation. The International Journal of Artificial Organs. 2014; 37(3):187-205. [DOI:10.5301/ijao.5000307] [PMID]

[24] Gentile P, Chiono V, Carmagnola I, Hatton PV. An overview of poly (lactic-co-glycolic) acid (PLGA)-based biomaterials for bone tissue engineering. International Journal of Molecular Sciences. 2014; 15(3):3640-59. [DOI:10.3390/ijms15033640] [PMID] [PMCID]

[25] Benatti AC, Pattaro AF, Rodrigues AA, Xavier MV, Kaasi A, Barbosa MI, et al. Bioreabsorbable polymers for tissue engineering: PLA, PGA, and their copolymers. In: Materials for biomedical engineering. Amsterdam: Elsevier; 2019. [DOI:10.1016/B978-0-12-816901-8.00004-3]

[26] Satchanska G, Davidova S, Petrov PD. Natural and synthetic polymers for biomedical and environmental applications. Polymers. 2024; 16(8):1159. [DOI:10.3390/polym16081159] [PMID] [PMCID]

[27] Jung K, Corrigan N, Wong EH, Boyer C. Bioactive synthetic polymers. Advanced Materials. 2022; 34(2):2105063. [DOI:10.1002/adma.202105063] [PMID]

[28] Benalaya I, Alves G, Lopes J, Silva LR. A review of natural polysaccharides: sources, characteristics, properties, food, and pharmaceutical applications. International Journal of Molecular Sciences. 2024; 25(2):1322. [DOI:10.3390/ijms25021322] [PMID] [PMCID]

[29] Sharma R, Malviya R, Singh S, Prajapati B. A critical review on classified excipient sodium-alginate-based hydrogels: modification, characterization, and application in soft tissue engineering. Gels. 2023; 9(5):430. [DOI:10.3390/gels9050430] [PMID] [PMCID]

[30] Spicer CD. Hydrogel scaffolds for tissue engineering: the importance of polymer choice. Polymer Chemistry. 2020; 11(2):184-219. [DOI:10.1039/C9PY01021A]

[31] Elices M. Structural biological materials: Design and structure-property relationships. Oxford: Pergamon; 2000. [Link]

[32] Bignami A, Hosley M, Dahl D. Hyaluronic acid and hyaluronic acid-binding proteins in brain extracellular matrix. Anatomy and Embryology. 1993; 188(5):419-33. [DOI:10.1007/BF00190136]

[33] Necas J, Bartosikova L, Brauner P, Kolar J. Hyaluronic acid (hyaluronan): A review. veterinary Medicine Journal. 2008; 53(8):397-411. [DOI:10.17221/1930-VETMED]

[34] Gupta RC, Lall R, Srivastava A, Sinha A. Hyaluronic acid: Molecular mechanisms and therapeutic trajectory. Frontiers in Veterinary Science. 2019; 6:192. [DOI:10.3389/fvets.2019.00192] [PMID] [PMCID]

[35] Grinkova AA, Ustyuzhanina NE, Nifantiev NE. Synthesis of oligosaccharides structurally related to hyaluronic acid fragments. Russian Journal of Bioorganic Chemistry. 2022; 48(2):191-220. [DOI:10.1134/S1068162022020108]

[36] Iqbal M, Yasin A, Akram A, Li JA, Zhang K. Advances of sulfonated hyaluronic acid in biomaterials and coatings-A review. Coatings. 2023; 13(8):1345. [DOI:10.3390/coatings13081345]

[37] Snetkov P, Zakharova K, Morozkina S, Olekhnovich R, Uspenskaya M. Hyaluronic acid: The influence of molecular weight on structural, physical, physico-chemical, and degradable properties of biopolymer. Polymers. 2020; 12(8):1800. [DOI:10.3390/polym12081800] [PMID] [PMCID]

[38] Zhao N, Wang X, Qin L, Zhai M, Yuan J, Chen J, et al. Effect of hyaluronic acid in bone formation and its applications in dentistry. Journal of Biomedical Materials Research Part A. 2016; 104(6):1560-9. [DOI:10.1002/jbm.a.35681] [PMID]

[39] Bowman S, Awad ME, Hamrick MW, Hunter M, Fulzele S. Recent advances in hyaluronic acid based therapy for osteoarthritis. Clinical and Translational Medicine. 2018; 7(1):6. [DOI:10.1186/s40169-017-0180-3] [PMID] [PMCID]

[40] Yang H, Song L, Zou Y, Sun D, Wang L, Yu Z, et al. Role of hyaluronic acids and potential as regenerative biomaterials in wound healing. ACS Applied Bio Materials. 2020; 4(1):311-24. [DOI:10.1021/acsabm.0c01364] [PMID]

[41] Jia W, Liu L, Li M, Shen Q, Qi G, Zhou R, et al. Hyaluronic acid oligosaccharides promote micro-vessel growth and regenerative ossification in biomimetic calvarial bone scaffolds. Acta Biomaterialia. 2025; 208:254-65. [DOI:10.1016/j.actbio.2025.10.042] [PMID]

[42] Rana MM, De la Hoz Siegler H. Evolution of hybrid hydrogels: Next-generation biomaterials for drug delivery and tissue engineering. Gels. 2024; 10(4):216. [DOI:10.3390/gels10040216] [PMID] [PMCID]

[43] Chen H, Xue H, Zeng H, Dai M, Tang C, Liu L. 3D printed scaffolds based on hyaluronic acid bioinks for tissue engineering: A review. Biomaterials Research. 2023; 27(1):137. [DOI:10.1186/s40824-023-00460-0] [PMID] [PMCID]

[44] Liu Q, Ding J, Mante FK, Wunder SL, Baran GR. The role of surface functional groups in calcium phosphate nucleation on titanium foil: A self-assembled monolayer technique. Biomaterials. 2002; 23(15):3103-11. [DOI:10.1016/S0142-9612(02)00050-9] [PMID]

[45] Hablee S, N. Razali N, SF Alqap A, Sopyan I. Recent developments on injectable calcium phosphate bone cement. Recent Patents on Materials Science. 2016; 9(2):72-94. [DOI:10.2174/1874464809666160802145629]

[46] Arita K, Yamamoto A, Shinonaga Y, Harada K, Abe Y, Nakagawa K, et al. Hydroxyapatite particle characteristics influence the enhancement of the mechanical and chemical properties of conventional restorative glassionomer cement. Dental Materials Journal. 2011; 30(5):672-83. [DOI:10.4012/dmj.2011-029] [PMID]

[47] Chen YH, Chung YC, Wang IJ, Young TH. Control of cell attachment on pH-responsive chitosan surface by precise adjustment of medium pH. Biomaterials. 2012; 33(5):1336-42. [DOI:10.1016/j.biomaterials.2011.10.048] [PMID]

[48] Alkhraisat MH, Rueda C, Marino FT, Torres J, Jerez LB, Gbureck U, et al. The effect of hyaluronic acid on brushite cement cohesion. Acta Biomaterialia. 2009; 5(8):3150-6. [DOI:10.1016/j.actbio.2009.04.001] [PMID]

[49] George A, Veis A. Phosphorylated proteins and control over apatite nucleation, crystal growth, and inhibition. Chemical Reviews. 2008; 108(11):4670-93. [DOI:10.1021/cr0782729] [PMID] [PMCID]

[50] Rahul AV, Sharma A, Santhanam M. A desorptivity-based approach for the assessment of phase separation during extrusion of cementitious materials. Cement and Concrete Composites. 2020; 108:103546. [DOI:10.1016/j.cemconcomp.2020.103546]

[51] Asah D, Raju S, Ghosh S, Mukhopadhyay S, Mehta AC. Nonthrombotic pulmonary embolism from inorganic particulate matter and foreign bodies. Chest. 2018; 153(5):1249-65. [DOI:10.1016/j.chest.2018.02.013] [PMID]

[52] Lasheras-Zubiate M, Navarro-Blasco I, Fernández JM, Alvarez JI. Studies on chitosan as an admixture for cement-based materials: Assessment of its viscosity enhancing effect and complexing ability for heavy metals. Journal of Applied Polymer Science. 2011; 120(1):242-52. [DOI:10.1002/app.33048]

[53] Konishi T, Honda M, Nagaya M, Nagashima H, Thian ES, Aizawa M. Injectable chelate-setting hydroxyapatite cement prepared by using chitosan solution: fabrication, material properties, biocompatibility, and osteoconductivity. Journal of Biomaterials Applications. 2017; 31(10):1319-27. [DOI:10.1177/0885328217704060] [PMID]

[54] Dorozhkin SV. Calcium orthophosphate cements and concretes. Materials. 2009; 2(1):221–91. [DOI:10.3390/ma2010221]

[55] Zhang Y, Zhang M. Synthesis and characterization of macroporous chitosan/calcium phosphate composite scaffolds for tissue engineering. Journal of Biomedical Materials Research. 2001; 55(3):304-12. [DOI:10.1002/1097-4636(20010605)55:3<304::aid-jbm1018>3.0.co;2-j] [PMID]

[56] Kretlow JD, Mikos AG. Review: Mineralization of synthetic polymer scaffolds for bone tissue engineering. Tissue Engineering Part A: Research Advances. 2007; 13(5):927-38. [DOI:10.1089/ten.2006.0394] [PMID]